FISSURE-BLOCK MODEL FOR TRANSIENT PRESSURE ANALYSIS IN GEOTHERMAL STEAM RESERVOIRS

A.F. Moench, USGS, Menlo Park, CA
R. Denlinger, USGS, Denver, CO

Introduction

The fissure-block model considered in this paper is sometimes called a dual-porosity model or a naturally fractured reservoir model. Ground water and petroleum literature commonly refer to the pioneering analytical work on this subject by Barenblatt and others (1960) and Warren and Root (1963). These early papers consider flow from primary porosity blocks to secondary porosity fissures but they do not describe the flow within these blocks. Kazemi (1969) presents a finite-difference solution for single-phase flow which does account for flow within the blocks and Boulton and Streltsova (1977) give exact solutions for this problem.

At an earlier Stanford workshop, Moench (1978) presented a nonisothermal, radial flow, fissure-block, finite-difference model for geothermal steam reservoirs which was later used to simulate pressure buildup data for a steam well in Larderello, Italy (Moench and Neri, 1979). The model assumed the blocks to be impermeable but capable of conducting heat to the fissures which had been cooled by vaporization. In the present paper the model is revised to account for steam transport and vaporization within the blocks. This is a necessary consideration in order to account for the longevity of production wells in The Geysers. The blocks, which may be initially saturated with liquid water, are assumed to have low intrinsic permeability and low porosity relative to the fissures.

Results computed with this finite-difference model are compared, for isothermal conditions, with the solutions of Boulton and Streltsova (1977). Under these conditions the model is similar to that of Kazemi (1969). When vaporization occurs in the blocks from a small amount of uniformly-distributed liquid water it is also possible to apply Boulton and Streltsova's solutions. This is done by allowing for the apparent compressibility of the two-phase fluid mixture in the block. Comparison with Boulton and Streltsova's solutions under two-phase conditions is given in order to verify the finite-difference code.

Numerical results are also presented showing pressure buildup following production with the blocks initially nearly saturated with liquid water. Effects of different thermal boundary conditions, block sizes and production times on pressure buildup curves are examined.

After further refinements the model will be calibrated, using available pressure buildup data from representative wells in The Geysers, and used to provide a means for estimating pore pressure and temperature gradients within reservoir blocks. This information will be used to calculate changes in effective stress in the vicinity of a boiling front: a mechanism proposed to account for earthquake activity in the vicinity of The Geysers (Denlinger and Moench, 1979).

Approach

The conceptual model illustrated in figure 1a is idealized as shown in figure 1b. Alternating layers of fissures and blocks of constant thickness are assumed to extend radially to infinity. The thickness of the fissure and block is assumed to represent the average thickness of the fissures and blocks in the reservoir. In the model radial flow in the fissure is coupled with one-dimensional planar flow in the blocks perpendicular to the fissures. With the onset of well discharge, pressure reductions in the fissure induce vaporization of liquid water in the blocks. Liquid in the fissures and blocks is assumed to be immobile. This assumption is justified for the blocks by their low porosity and for the fissures by their low liquid saturation. Large capillary forces brought about by these conditions are assumed to hold the liquid in place. Saturations, therefore, change only in response to vaporization or condensation. The relative permeability to steam is assumed to change with liquid saturation in accordance with the Corey (1954) relationship.

Equations for the radial flow of steam through porous reservoirs in the presence of immobile vaporizing or condensing liquid water are given by Moench and Atkinson (1978). It was assumed in that study that the only temperature changes that take place in the reservoir are those due to phase change: conduction, convection, and pressure-work are considered negligible by comparison. In this paper heat is conducted from the fissure into the block or vice versa. Temperature changes in the block occur in response to both phase change and heat conduction. The exterior ($Z=H$) thermal boundary of the block is assumed to be either constant temperature or insulating. The exterior flow boundary of the block is assumed to be no flow.

A finite-difference code is used to compute pressure, temperature, and saturation changes at each node in the fissure and block. These computations are carried out in the manner described by Moench and Atkinson (1978) with the added dimension that planar flow in the block is computed for as many vertical arrays as there are nodes in the fissure. Fissure nodes serve as boundaries for the block arrays. The distance between the nodes in the block is increased logarithmically with distance from the fissure in the same way as the nodes in the fissure become more widely separated with distance from the well.

Model Verification

Exact solutions for single-phase flow in a fissure-block system by Boulton and Streltsova (1977) are used in this study to validate the results of the finite-difference model. Their solutions are presented in the form of semi-infinite integrals which are quite difficult to solve numerically. However in the Laplace transformed space the solutions appear in a simpler form and can be inverted numerically by the method of Stehfest (1970). The results so obtained will be referred to as the analytical solutions.

The Laplace transform solution for pressure drawdown in the fissure appears as follows:

$$\bar{P}_{D1} = \frac{K_o(r_D k)}{s} \tag{1}$$

where $$k = \sqrt{\eta^2 \frac{\alpha_2}{\alpha_1} + \eta \frac{T_2}{T_1} \frac{r_w}{H} \tanh\left(\eta \frac{H}{r_w}\right)}$$

$$\eta = \sqrt{\frac{s r_w^2}{\alpha_2}}, \quad T_1 = k_1 h, \quad T_2 = k_2 H$$

Symbols are defined in Table 1.

The Laplace transform solution for pressure drawdown in the block appears as follows:

$$\bar{P}_{D2} = A \frac{K_o(r_D k)}{s} \tag{2}$$

where $A = \cosh\left(\eta \frac{Z}{r_w}\right) - \tanh\left(\eta \frac{H}{r_w}\right) \cdot \sinh\left(\eta \frac{Z}{r_w}\right)$

Figure 2 shows a comparison of the analytical and numerical results for dimensionless pressure drawdown (P_D vs log t_D) at the well bottom and at a specified point within the block for single-phase steam. Parameters required for the comparison are given in Table 1. The deviation in the results which is most apparent at an early time can be attributed primarily to spatial descretization at the block-fissure contact. Care was taken in the numerical model to reduce nonlinearities by avoiding large pressure changes.

The model of Boulton and Streltsova (1977) can also be used to validate the finite-difference model for vaporization in the reservoir block. With immobile liquid water distributed uniformly throughout the block, the liquid-steam combination in the block can be considered to have an enhanced compressibility. The amount by which the compressibility is enhanced can be calculated as shown in the appendix using the equations of either Grant and Sorey (1979) or Moench and Atkinson (1978).

Figure 3 shows the results obtained when a small amount of liquid water (S_i=0.01) is introduced in the block. Because of the increased compressibility, the ratio of diffusivities between the fissure and block is increased over that which applies to the results in figure 2 by a factor of 430 (see appendix). This causes the pressure response shown in figure 3 to be shifted toward larger values of dimensionless times. The displacement between the finite-difference and the analytical results can again be attributed to discretization at the block-fissure contact. In figure 3 however there is, in addition, a lack of pressure support in the finite-difference model which results from the fact that no vaporization occurs at the "fissure" node of the block array; hence the computed pressure drawdown is greater than indicated by the analytical solution. In view of the magnitude of the change in pressure response over that shown in figure 2, brought about simply by introducing liquid in the block, the authors feel that the agreement with the analytical solution is adequate and that the model has been validated by these results.

Results

Computer runs were made to simulate hypothetical conditions using different parameters. Results are presented that illustrate the variations in pressure buildup that can be expected when thermal boundary conditions, block size, or production time are changed. In all cases the block was assumed to have very low porosity and permeability relative to the fissure and an initial liquid-water content close to saturation. Hydraulically connected steam is considered the more mobile phase even under these conditions because liquid water, as the wetting phase, can be assumed to be held in place by capillary forces. This assumption is supported in part by the work of Chen and others (1978) who found by experimentation that a core with porosity of 34 percent and a permeability of 36 md appeared to have a practical irreducible liquid-water saturation in excess of 60 percent. Parameters used in the simulations are given in Table 2.

Figure 4 shows the pressure buildup at the well bottom after 1666 h (69 days) of production for a case in which the exterior boundary of the block (Z=H) is maintained at the initial reservoir temperature. The block itself is cooled by vaporization during production but is reheated by conduction. In figure 4 sufficient time has elapsed during production for temperatures in the block and fissure to have very nearly recovered to the initial reservoir temperature. The early time pressure buildup is due to the flow of superheated steam. After about one hour the pressure has recovered close to the initial reservoir pressure after which condensation commences.

Figure 5 shows pressure buildup for three different production times using the same parameters as shown in figure 4 but with the inner boundary of the block thermally insulated. This is considered a more realistic possibility in a fissured reservoir. The figure shows a systematic downward progression of the

pressure buildup curves as production time increases. After 4015 h (167 days) of production all the liquid in the block near the well has vaporized and the block and fissure have cooled to the point where steam at the well bottom is only slightly superheated. Consequently, almost immediately after shut in, condensation occurs in the fissure. The shape of the buildup curve after that is the result of condensation in both the fissure and block and the dissipation of latent heat by conduction. When the same well is produced for shorter times not as much cooling occurs in the block and fissure and consequently condensation occurs at higher pressures. When the well is produced for only 78 hours the fissure still retains much of the heat it had initially because it has not had time to cool by conduction into the block. As a consequence the early portion of the pressure buildup curve exhibits effects of superheating.

Figure 6 shows pressure buildup after a production time of 1130 h (47 days) using the same conditions as in figure 5 except that the thickness of the block is increased and the production rate is doubled. The pressure buildup in the first 30 minutes after shut in is due to the flow of superheated steam.

Figures 4-6 show the variability that can be expected in the shape of pressure buildup curves when model parameters are varied. It can be inferred from these results that the degree to which vaporization has depleted the liquid in the block has an important bearing upon the shape of the curves. These factors should be considered when interpreting pressure buildup tests in steam reservoirs.

References

Barenblatt, G.E., Zheltov, I.P., and Kochina, I.N.: "Basic concepts in the theory of seepage of homogeneous liquids in fissured rocks, " Journal of Applied Mathematics and Mechanics (1960). 24, 1286-1303.

Boulton, N.S., and Streltsova, T.D.: "Unsteady flow to a pumped well in a fissured water-bearing formation," J. Hydrol. (1977), 35, 257-270.

Chen, H.K., Counsil, J.R., and Ramey, H.J., Jr.: "Experimental steam-water relative permeability curves," Geothermal Resources Council, Transactions (1978), 2, 103-104.

Corey, A.T.: "The interrelation between gas and oil relative permeabilities": Producers Monthly (1954), 19, 38-41.

Denlinger, R. and Moench, A.F.: "Stress changes due to fluid depletion at The Geysers steam field in Northern California (abstract)," A.G.U. Fall Meeting (1979), EOS 60 (46), 946.

Grant, M.A., and Sorey, M.L.: "The compressibility and hydraulic diffusivity of a water-steam flow," Water Resources Research (1979), 15(3), 684-686.

Kazemi, H.: "Pressure transient analysis of naturally fractured reservoirs with uniform fracture distribution," Soc. Pet. Eng. J. (Dec 1969), 9, 451-462.

Moench, A.F.: "The effect of thermal conduction upon pressure drawdown and buildup in fissured, vapor-dominated geothermal reservoirs," Proc. Fourth Workshop on Geothermal Reservoir Engineering, Stanford University, Stanford, CA (1978), 112-117.

Moench, A.F. and Neri, G.: "Analysis of Gabbro I - steam pressure buildup test," Proc. Fifth Workshop on Geothermal Reservoir Engineering, Stanford University, Stanford, CA (1979), 99-104.

Moench, A.F., and Atkinson, P.G.: "Transient pressure analysis in geothermal steam reservoirs with an immobile vaporizing liquid phase," Geothermics (1978), 7, 253-264.

Stehfest, H.: "Numerical inversion of Laplace transforms," Commun. of the ACM (1970), 13(1), 47-49.

Warren, J.E., and Root, P.J.: "The behavior of naturally fractured reservoirs," Soc. Pet. Eng. J. (Sept. 1963), 3, 245-455.

Nomenclature

c_t	steam compressibility
C_D	well bore storage
H_c	reservoir heat capacity
H	block half thickness
h	fissure half thickness
K_o	modified Bessel function, 2nd kind, zero order
K	thermal conductivity
k	permeability
k_s	skin permeability
L_v	latent heat of vaporization
M_w	molecular weight of water
P_D	$\frac{\pi k h M_w}{q \mu_v Z_i R T} (P_i^2 - P^2)$
P_i	initial pressure
P	pressure
q	production rate
r_D	r/r_w
r_w	well radius
r	radial dimension
Δr_s	skin thickness
R	gas constant
S_i	initial liquid saturation
s	Laplace transform variable
t_D	$\frac{k_1 t}{\phi_1 \mu_v c_t r_w^2}$
t	time
Z_i	initial compressibility factor
z	planar dimension in block
α	fluid diffusivity
β	steam thermal expansivity
μ_v	steam viscosity
ρ_v	steam density
ϕ	porosity

subscripts

1	fissure
2	block
D	dimensionless

Appendix

Following the discussion given by Moench and Atkinson (1978) the diffusivity of the steam in the fissure is given by:

$$\alpha_1 = \frac{k_1}{\phi_1 \mu_v c_t} \quad , \tag{A1}$$

and the diffusivity of the steam-liquid combination in the block is given by:

$$\alpha_2 = \frac{k_2}{\phi_2 \mu_v c_t (1+A)} \tag{A2}$$

where $$A = \frac{H_c}{L_v} \frac{dT}{dP} \frac{1}{\phi_2 \rho_v c_t} - \frac{\beta}{c_t} \frac{dT}{dP}$$

If there is no liquid in the block A=0. Neglecting the relatively small effects of steam compressibility, specific heat, and thermal expansivity the combination of terms $c_t(1+A)$ become equivalent to the approximate total compressibility, β_t, given by Grant and Sorey (1979). They give a useful expression for $\phi\beta_t$ which is a function of pressure and reservoir heat capacity:

$$\phi_2 \beta_t = 1.92 \times 10^{-5} H_c P^{-1.66} \tag{A3}$$

where P is in bars and H_c is in $J/m^{3\circ}C$.

The ratio of diffusivity in the fissure to that in the block thus appears as:

$$\frac{\alpha_1}{\alpha_2} = \frac{k_1}{k_2} \frac{\phi_2 \beta_t}{\phi_1 c_t} \tag{A4}$$

When only steam is present $\beta_t = c_t$ and for the parameters of figure 2 the ratio $\alpha_1/\alpha_2 = 10^3$. When liquid and steam coexist at 30 bars initial pressure, $\phi_2\beta_t = 0.172$ bar^{-1} and the ratio $\alpha_1/\alpha_2 = 430 \times 10^3$.

Table 1

Parameters used for comparison of model with analytical solutions*

H_{c1}	0.55 cal/°C cm^3	q	2.77 g/s
H_{c2}	0.61 cal/°C cm^3	r_w	16 cm
H	75 cm	S_{i1}	0.0
h	10 cm	S_{i2}	0.0, 0.1
K	0.0 cal/(°C cm sec)	T	234°C
k_1	10^{-8} cm^2	ϕ_1	0.1
k_2	$10^{-12}cm^2$	ϕ_2	0.01
P_i	30 bars		

Table 2

Parameters used for the pressure buildup simulations*

C_D	166	P_i	30 bars
H_{c1}	0.55 cal/°C cm^3	q	27.7 g/s, 55.4 g/s
H_{c2}	0.62 cal/°C cm^3	r_w	16 cm
H	104 cm, 374 cm	Δr_s	16 cm
h	10 cm	S_{i1}	0.0
K	0.006 cal/(cm sec °C)	S_{i2}	0.8
k_1	10^{-8} cm^2	T	234°C
k_2	10^{-13} cm^2	ϕ_1	0.1
k_3	10^{-7} cm^2	ϕ_2	0.01

*parameters not listed are known properties of water at prevailing temperature and pressure.

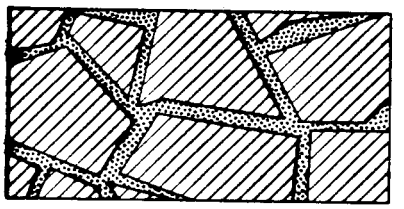

Figure 1a

Conceptual model with porous blocks and fissures

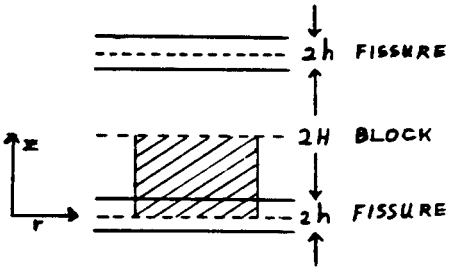

Figure 1b

Idealized fissure-block reservoir used in the analysis

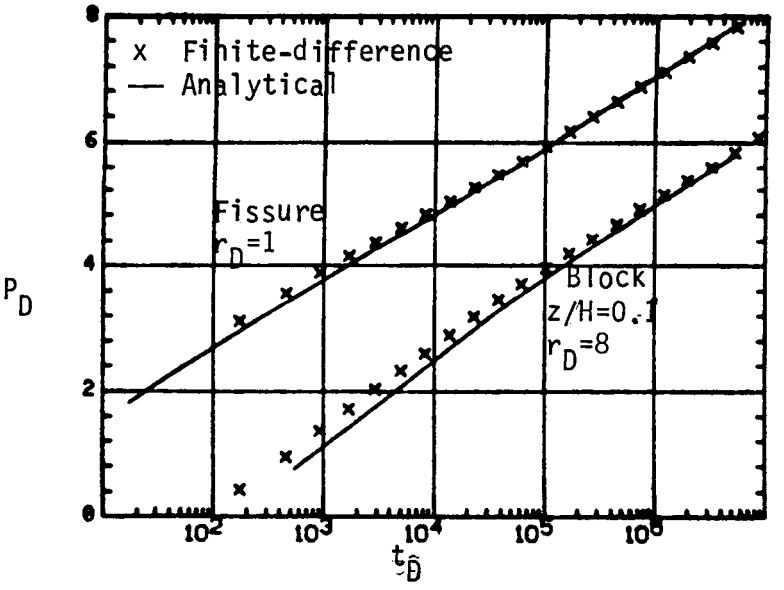

Figure 2

Comparison of analytical and numerical results for single phase steam in block and fissure.

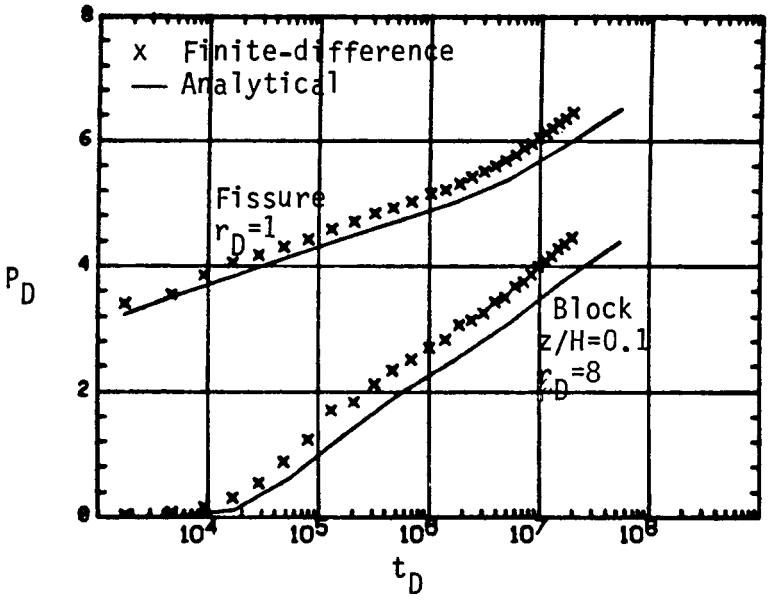

Figure 3

Comparison of analytical and numerical results with liquid and steam in the block and single-phase steam in fissure.

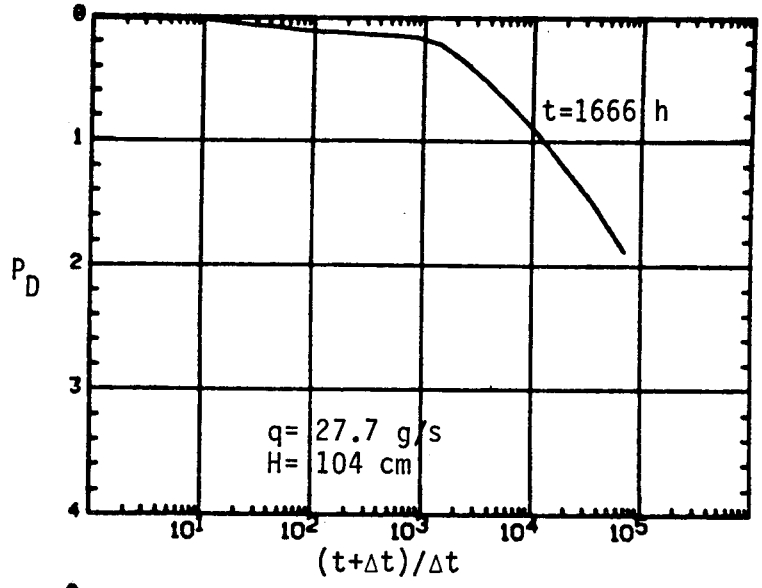

Figure 4

Pressure buildup at well bottom using constant temperature boundary in the block.

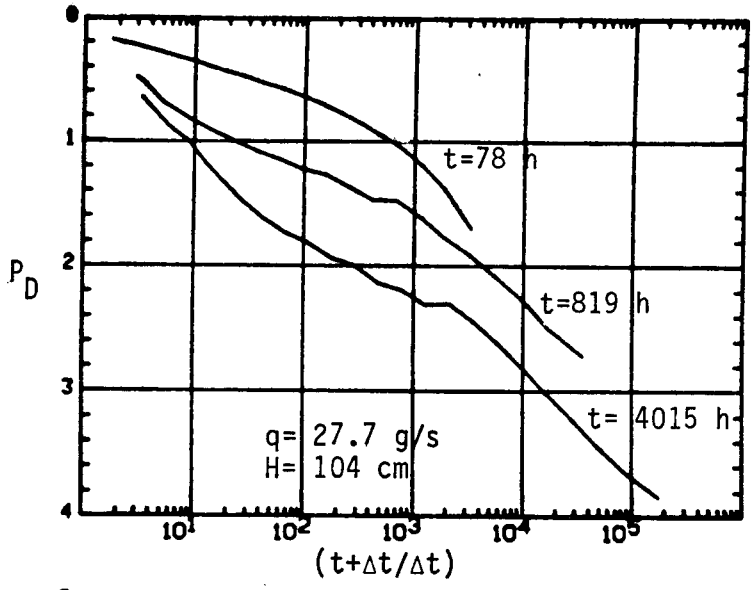

Figure 5

Pressure buildup at well bottom using thermally insulated boundary in the block.

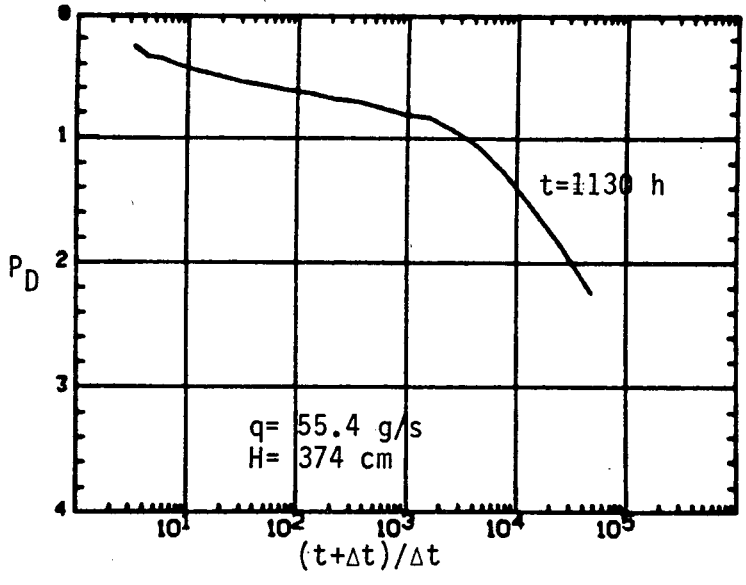

Figure 6

Pressure buildup at well bottom using thermally insulated boundary in the block.